Journal of Inorganic and Organometallic Polymers and Materials (2020) 30:359–368
https://doi.org/10.1007/s10904-019-01194-0

Fine Copper Nanoparticles on Amine Functionalized SBA-15 as an Effective Catalyst for Mannich Reaction and Dye Reduction

S. Anbu Anjugam Vandarkuzhali[1] · B. Viswanathan[1] · M. P. Pachamuthu[2] · S. Chandra Kishore[3]

Received: 29 March 2019 / Accepted: 15 May 2019 / Published online: 20 May 2019

Abstract

Copper nanoparticles dispersed on amine functionalised mesoporous silica SBA-15 (Cu/NH_2-SBA-15) were synthesised by a simple sol–gel and impregnation method using sodium borohydride ($NaBH_4$) as a reducing agent. The morphology, mesostructure and functionality of the ordered mesoporous Cu/NH_2-SBA-15 were evaluated by powder X-ray diffraction (PXRD), Scanning electron microscopy (SEM), Transmission electron microscopy (TEM), Nitrogen adsorption–desorption isotherms (BET) and Fourier transform infrared spectroscopy (FTIR). The results obtained revealed, that the amine functionalised SBA-15 holds hexagonal lamelliform with surface area and pore size of 250 m^2/g, 2.2 nm respectively. Moreover, these short vertical channels have a substantial role in the uniform dispersion of copper nanoparticles within the meso-channels of amine functionalised SBA-15. Cu nanoparticles in the size range of 4–7 nm were dispersed on the NH_2-SBA-15 support. To confirm the potential catalytic activity, Cu/NH_2-SBA-15 was tested in Mannich reaction. The catalyst showed an excellent catalytic activity for the yield (90%) of β-amino carbonyl compounds that serve as a building block for the synthesis of lactams, peptides, amino alcohols and precursor for various amino acids. Further, the activity of the catalyst was also tested for the reduction of dyes. The structural influence over the reduction pathways was studied on triphenyl methane dyes.

Graphical Abstract

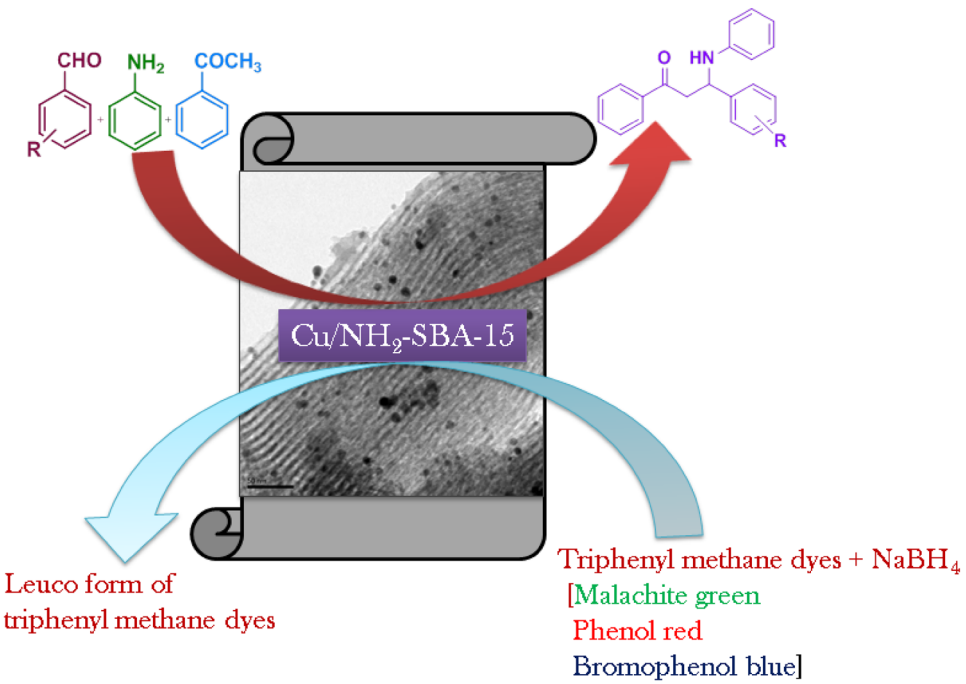

Extended author information available on the last page of the article

Keywords Copper nanoparticle · SBA-15 · Amine functionalization · Mannich reaction · Reduction of dyes

1 Introduction

Since the discovery of Mannich reaction by Carl Ulrich Franz Mannich in 1912, the synthesis of nitrogen containing molecules has gained immense attention in the field of organic chemistry research [1]. The product β-amino carbonyl compounds obtained in this reaction act as building block for the synthesis of lactams, peptides, amino alcohols and precursor for various amino acids [2–4]. In general, this is a carbon–carbon bond formation reaction that profoundly relies on a one pot three component reactants viz., amine, aldehyde and ketone set up rather than a known two component set up [5, 6]. There are several reports on this reaction involving conventional catalysts like Bronsted acids [7, 8], Lewis acid [9, 10], Lewis base [11] and transition metal salts [12, 13]. These catalysts indeed have some drawbacks such as leaching, recycling and reusability of the catalyst, long reaction time, tedious reaction conditions and wary product separation. In order to overcome these demerits, we have adopted a better remedy by interpolating a stable metal nanoparticle supported mesoporous catalyst for the Mannich reaction.

In general, the activity and reactivity of a catalytic reaction are mainly predicted based on particle size, surface structure, number of active sites and the position of metal centre. Copper based catalysts with these characteristics are considered as an excellent candidate for the Mannich reaction [14]. Compared to the bulk copper, reasonably available copper nanoparticles have an excellent feature of a heterogeneous catalyst with high surface to volume ratio that can develop more active sites for the reaction [15]. This eventually led to exceptional physical and chemical properties. Despite of these merits conventional supported catalysts prepared by wet chemical methods have very less dispersed active sites. An economical and simple protocol for large dispersion of these nanoparticles always remains as a challenging task for the researchers.

The discovery of mesoporous silica materials viz., MCM-41, SBA-15, TUD-1, KIT-6 has opened avenues for its exploitation as catalyst support [16–21]. Among these mesoporous material, SBA-15 is of great interest because of high surface area (600–1000 m^2/g), tunable hexagonal pore (5–30 nm) with long uniform channels [22]. There are various reports on the synthesis and application of Cu loaded mesoporous materials [23–25]. Tailoring the particle size of Cu nanoparticles with higher loading to fill the nanopores of SBA-15 materials is considered difficult because of the agglomeration of these particles due to sintering. Modification of SBA-15 with amine functionalisation can solve this problem by binding the Cu^0 nanoparticles on the surface of support which indirectly prevent leaching thereby enhancing the reusability and recycling efficiency of the catalyst. Thus, in order to attain higher yield by overcoming the demerits of the conventional catalyst we have used copper nanoparticles dispersed on amine functionalised SBA-15 mesoporous catalyst (Cu/NH_2-SBA-15) to perform Mannich reaction. To the best of our knowledge there is no report on Cu/NH_2-SBA-15 for Mannich reaction. In addition, the thicker pore wall with high thermal and mechanical stability, fixation of large active complex, reduced diffusional restriction of the reactants makes Cu/NH_2-SBA-15 as excellent candidate for the Mannich reaction with high yield. Moreover, the efficiency of the catalyst was tested for the reduction of selected triphenyl methane dyes (Malachite green (MG), phenol red (PR), and bromophenol blue (BPB)).

2 Materials and Methods

2.1 Chemicals

Pluronic P123 ($EO_{20}PO_{70}EO_{20}$), hydrochloric acid (HCl), tetraethylorthosilicate (TEOS), toluene, 3-aminopropyltrimethoxysilane [APTMS, $(H_2N(CH_2)_3–Si(OMe)_3)$], copper nitrate [$Cu(NO_3)_2{\cdot}6H_2O$], sodium borohydride ($NaBH_4$), acetophenone, benzaldehyde and aniline, malachite green, bromophenol blue, phenol red are purchased from Sigma Aldrich and Merck.

2.2 Catalyst Preparation

2.2.1 Synthesis of SBA-15 Mesoporous Silica

Mesoporous SBA-15 was synthesized according to the previous report by Zhao et al. [26]. Briefly, 4 g of pluronic P123 ($EO_{20}PO_{70}EO_{20}$) as template and hydrochloric acid 1 M HCl solution were subjected to magnetic stirring in a polypropylene bottle at 35 °C until P123 get dissolved completely. Later, 8.5 g of tetraethylorthosilicate (TEOS) was added dropwise and continuously stirred for 24 h. Upon formation of gel, the polypropylene was closed air tight with Teflon tape and heated at 100 °C for 48 h in an oven under static condition. The resulting white solid was dried and calcined at 550 °C for 6 h in a muffle oven to remove the organic template and used for the amine functionalization.

2.2.2 Synthesis of NH_2-SBA-15 Mesoporous Silica

For amine (NH_2) functionalization, calcined SBA-15 was pretreated at 150 °C for 2 h in a nitrogen atmosphere. The

pretreated SBA-15 was suspended in dry toluene (150 mL) and stirred for 30 min at 30 °C. Further, 2 ml of 3-aminopropyltrimethoxysilane [APTMS, $(H_2N(CH_2)_3–Si(OMe)_3)$] in 50 mL of toluene was added drop-wise to the slurry and stirred under reflux at 100 °C in an oil bath for 24 h. Finally, the product was then filtered, washed with ethanol, dried at 80 °C and stored in a vacuum desiccator. The sample is represented as NH_2-SBA-15.

2.2.3 Synthesis of Cu/NH_2-SBA-15

The copper nitrate ($Cu(NO_3)_2·6H_2O$) was used as the metal precursor for the synthesis of Cu nanoparticles. The solution of copper nitrate (20 mL, 0.1 M) was prepared by weighing the required amounts of metal salt in milli Q water. Required amounts of NH_2-SBA-15 sample was added to the above solutions and sonicated for 4 h at room temperature. The slurry obtained at the end of the reaction was filtered and the precipitate was vacuum dried. Ultrasonic reduction of metal precursors was performed by drop wise addition of a sodium borohydride ($NaBH_4$, 1 M) solution. After stirring for 30 min the precipitate obtained was filtered and dried under vacuum. The obtained bluish green colour solid is denoted as Cu/NH_2-SBA-15.

2.3 Catalyst Characterization

The powder X-ray diffraction (PXRD) patterns were recorded at room temperature using a Rigaku diffractometer with a nickel filtered Cu Kα (λ = 1.5418 Å) radiation source. N_2 sorption isotherms were recorded for the catalysts using Quantochrome porosimeter (*QuadrasorbSI*) at − 196 °C. High resolution transmission electron microscopy (HRTEM) was performed on FEI Tecnai G2 fitted with a CCD camera. The sample morphologies were examined using high resolution scanning electron microscope (HR-SEM) – FEI Quanta FEG 200 with low vacuum mode operation. FTIR spectra of KBr-diluted pellets of the sample were recorded on a Bruker instrument at room temperature with a resolution of 4 cm^{-1} averaged over 100 scans.

2.4 Synthesis of β-Amino Carbonyl Compounds

The Cu/NH_2-SBA-15 catalytic activity was tested for one pot three component reactions to synthesis the Mannich base. The 20 ml RB flask containing a mixture of acetophenone (1.0 mmol), benzaldehyde (1.0 mmol) and aniline (1.0 mmol) in methanol (5 ml) was added to Cu/NH_2-SBA-15 (50 mg) catalyst which was preheated at 100 °C for 2 h. The mixture was stirred at 30 °C for required time in a magnetic stirrer with oil bath. After the reaction was completed (as monitored by TLC using petroleum ether/ethyl acetate), the solid product was filtered and washed with ethanol. Finally, the yield of the product was isolated and calculated. The structure of product is confirmed by ^{1}HNMR, ^{13}C NMR, FTIR and physical constant (m.pt).

$$\text{Isolated yield (\%)} = (\text{Product experimental yield}/\text{Theoretical yield}) \times 100$$

2.4.1 Spectroscopic Data of 1,3-Diphenyl-3-(Phenylamino) Propan-1-One

A White solid; mp 170 °C; FTIR (KBr, cm^{-1}): 3380, 3060, 3020, 2920, 2870, 1670, 1599, 1500, 1445, 1370, 1294, 1220, 1074, 993, 860, 750, 622; ^{1}H NMR-(500 MHz, $CDCl_3$): δ 3.56–3.42 (m, 2H), 5.03 (m, 1H), 6.62–6.56 (d, 2H), 6.82–6.67 (m, 1H), 7.08–7.15 (m, 2H), 7.21–7.33 (m, 4H), 7.54–7.58 (m, 2H), 7.90–7.94 (m, 2H); ^{13}C NMR (500 MHz, $CDCl_3$): 46.3, 54.9, 59.7, 118.1, 127.5, 128.4, 128.8, 133.4, 136.8, 147.0, 198.2.

2.5 Reduction of Dyes

The catalytic efficiency of the catalyst was tested for the reduction of triphenyl methane dyes. To understand the influence of the groups, present in the structure; triphenyl methane dyes MG, PR and BPB were taken as model class. The reduction reaction was carried out as reported in our previous work [27]. Catalyst (10 mg) was added to the dye solution (20 mg l^{-1}) along with sodium borohydride ($NaBH_4$) (10 mmol) in a quartz cell and the progress of the reduction reaction was monitored using a UV–visible spectrophotometer at the respective chromophoric wavelength (λ_{max}) of the dyes.

2.5.1 Reaction Kinetic Analysis

The kinetics of the reduction reaction was maintained as pseudo unimolecular condition by adding excess of $NaBH_4$. The reduction reaction was carried out at room temperature with fixed amount of the dyes and catalyst. The rate constant was calculated from the slopes of the plots of ln C_0/C versus time.

The rate constants and percentage of dye reduction were calculated using the following mathematical expressions:

$$\text{Percentage reduction} = \frac{\text{O.D Initial time } (C_0) - \text{O.D time t } (C_t)}{\text{O.D Initial time } (C_0)} \times 100$$

where C_0 is initial concentration of the dye solution, C_t is concentration remaining after reaction at time t.

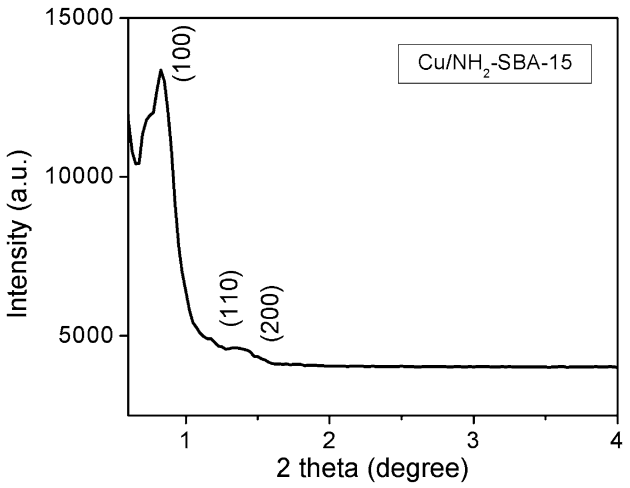

Fig. 1 Low angle XRD of Cu/NH_2-SBA-15

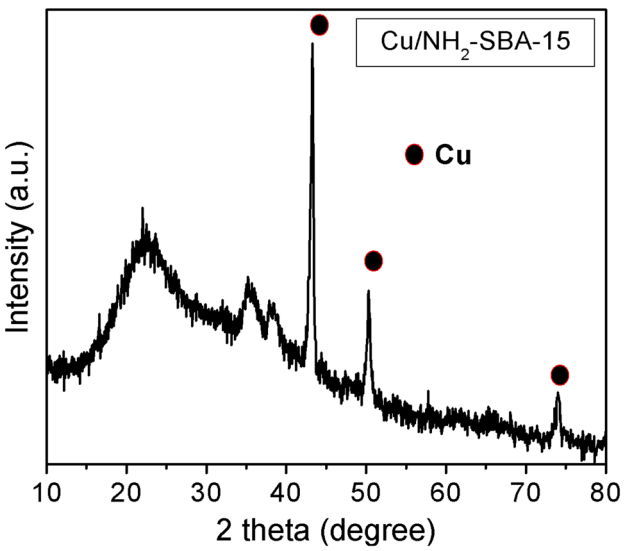

Fig. 2 High angle XRD Cu/NH_2-SBA-15

3 Results and Discussion

3.1 Catalyst Characterisations

Figure 1 shows the low angle powder X-ray diffraction patterns of Cu/NH_2-SBA-15 silica materials. The pattern exhibits three well-resolved characteristic peaks in the region 0.5°–2.51°, with a very strong intensity of (100) plane at $2\theta = 0.92$ representing the hexagonal mesostructure of SBA-15. The two weak intensity peaks indexed for (200) and (110) planes attributes to the finger print of 2D P6mm hexagonal symmetry and long-range order of the SBA-15 type materials [19, 28]. The intensity of the latter diffraction planes has decreased due to modification of pure SBA-15 by organic species ($–NH_2$) and Cu nanoparticles. The d_{100}-spacing (ca. 9.80 nm) of the mesopores framework, in the case of amine and Cu composites is observed to be, greater compared to the parent SBA-15 (ca. 9.02 nm), confirming the shrinkage of the mesoporous network due to the amine grafting and incorporation of metal nanoparticles within the pores.

The wide angle PXRD pattern of the mesoporous SBA-15 framework is depicted in Fig. 2. After the amine functionalization the characteristic reflections at 22° and 31° corresponding to amorphous silica seems unaffected, confirming that no damage has occurred due to amine grafting. Cu/NH_2-SBA-15 loaded with 10 wt% Cu over SBA-15 showed four prominent sharp diffraction peaks at 43.2°, 50.29°, 65.7° and 74.2° representing the (111), (200), (200) and (311) planes respectively, the cubic phase of Cu [JCPDS No. 04-0836] [25]. It can be inferred that the incorporation of the metal and amino-organic moieties does not affect the interplanar spacing of the material. The average grain size of Cu/NH_2-SBA-15 nanocomposites calculated using Debye–Scherrer formula is found to be ~2.6 nm for Cu nanoparticles.

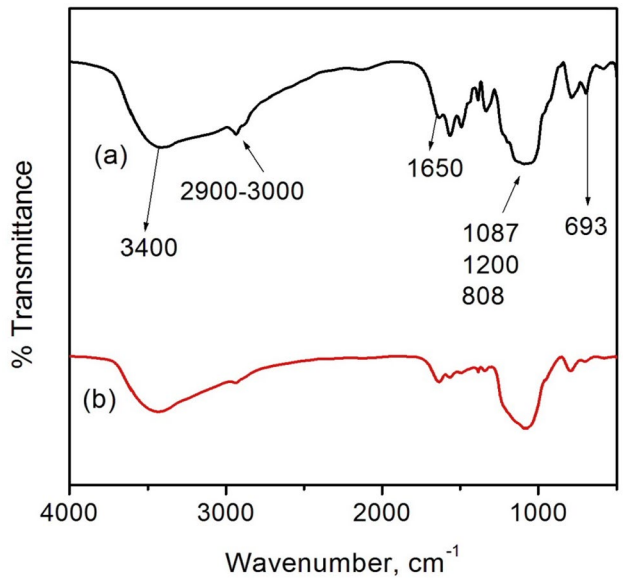

Fig. 3 FT-IR spectra of **a** NH_2-SBA-15 and **b** Cu/NH_2-SBA-15 catalysts

Besides, peaks at 35.5° and 38.6° corresponding to CuO nanoparticles [29], confirms the presence of CuO and Cu^0 species in Cu/NH_2-SBA-15 catalyst.

The FTIR spectra of pure SBA-15 and Cu/NH_2-SBA-15 are shown in Fig. 3. Presence of amine functionalization was confirmed from broad intense peak at 3500–3300 cm^{-1}. The broadness of the peak is due to the superimposition of the silanol (Si–OH) and amine ($–NH_2$) groups with cross linking hydrogen bonding [30]. Bands at 800 cm^{-1} is assigned for symmetric stretching vibration of Si–O–Si [30]; whereas the strong and broad peak at 1087 cm^{-1} is

attributed to the intense asymmetric stretching mode of Si–O covalent bond vibration. Also, the bending modes present at ~ 497 cm^{-1} confirms the presence of SBA-15 framework [31]. No traces of CuO in Cu/NH_2-SBA-15 were confirmed from the non-appearance of Cu–O stretch vibration band at 536 cm^{-1} [32]. Presence of C-H stretching bands in the organosilane framework can be observed in the range 3000-2800 cm^{-1} while stretching and deformation of NH frequencies are evident from 1590 cm^{-1} [33]. In addition, the bands at 1480 cm^{-1} and 687 cm^{-1} depicts the presence of $–NH_3^+$ frequency and N–H bending vibrations respectively [33]. Bands at 1605 and 2926 cm^{-1} are due to N–H bending and methylene vibrations, confirming that the amino groups are confined within the SBA-15 pore channels rather than the surface. The decrease in the intensities of absorption bands of Si–O–Si at 808 cm^{-1} indicates the presence of Cu nanoparticles within the pores of amine functionalized SBA-15.

The textural properties of Cu/NH_2-SBA-15 were studied using nitrogen physisorption isotherms Fig. 4a and b illustrates the adsorption/desorption isotherms and pore size distribution curves respectively. Cu/NH_2-SBA-15 exhibit a type IV isotherm with H2 hysteresis and a sharp increase in volume adsorbed at P/P_0 at higher relative pressure, suggesting the characteristic feature of highly ordered mesoporous materials with cylindrical and parallel pores [34]. The BET surface area of the calcined Cu/NH_2-SBA-15 was 250 m^2/g and the pore volume is 0.38 cm^3/g. These results well coincide with the XRD measurement and confirm the pore expansion due to the modification of silica structure and impregnation of Cu^0 in the silica surface. Using the BJH method the average pore size was calculated as 2.2 nm. It is evident that functionalisation of the SBA-15 did not affect the mesostructure of the same. Also, the presence of parallel hysteresis branches reveals the absence of pore plugging of metal oxide that normally exist in pore distribution curves as new maximum peak.

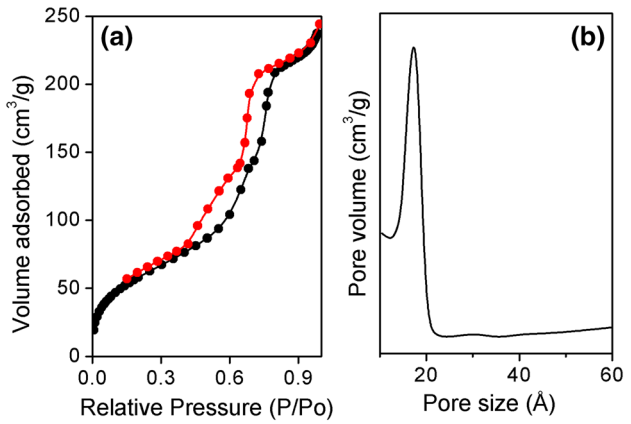

Fig. 4 **a** Nitrogen sorption and **b** pore size distribution of Cu/NH_2-SBA-15

Figure 5 shows the HRSEM image of Cu/NH_2-SBA-15. The micrograph indicates the well dispersed hexagonal particles arranged in fibre like morphology and aggregates of uniform rope-like particle with large fibrous structures with 10–20 µm in length and 2–4 µm in diameter. Noticeably, after copper dispersion, it is clearly observed from the micrographs, that the macroscopic aggregates resemble the original fibre like morphology; which corroborates with PXRD results.

Figure 6 represents the HRTEM images of Cu/NH_2-SBA-15. The presence Cu nanoparticles along the long channels of amine functionalized SBA-15 were evidenced by the presence of black spots along the pore channels in the micrographs. The regular hexagonal pore structure and long-range ordering with pore diameter of ~ 8 to 10 nm is observed in Fig. 6b. These Cu nanoparticles are found to be well dispersed inside the pores of NH_{-2}-SBA-15. The measured size of the nanoparticles is in the range of 5–10 nm. The presence of Cu species inside the channels

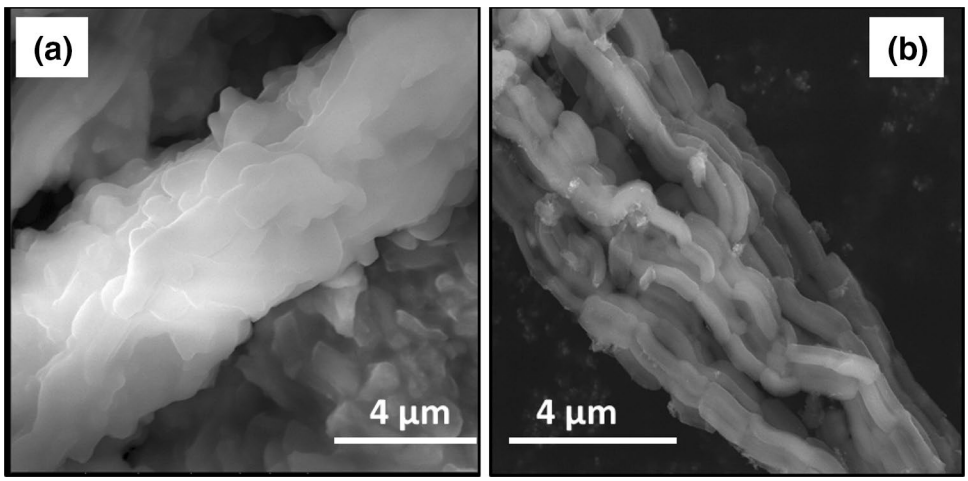

Fig. 5 SEM image of Cu/NH_2-SBA-15

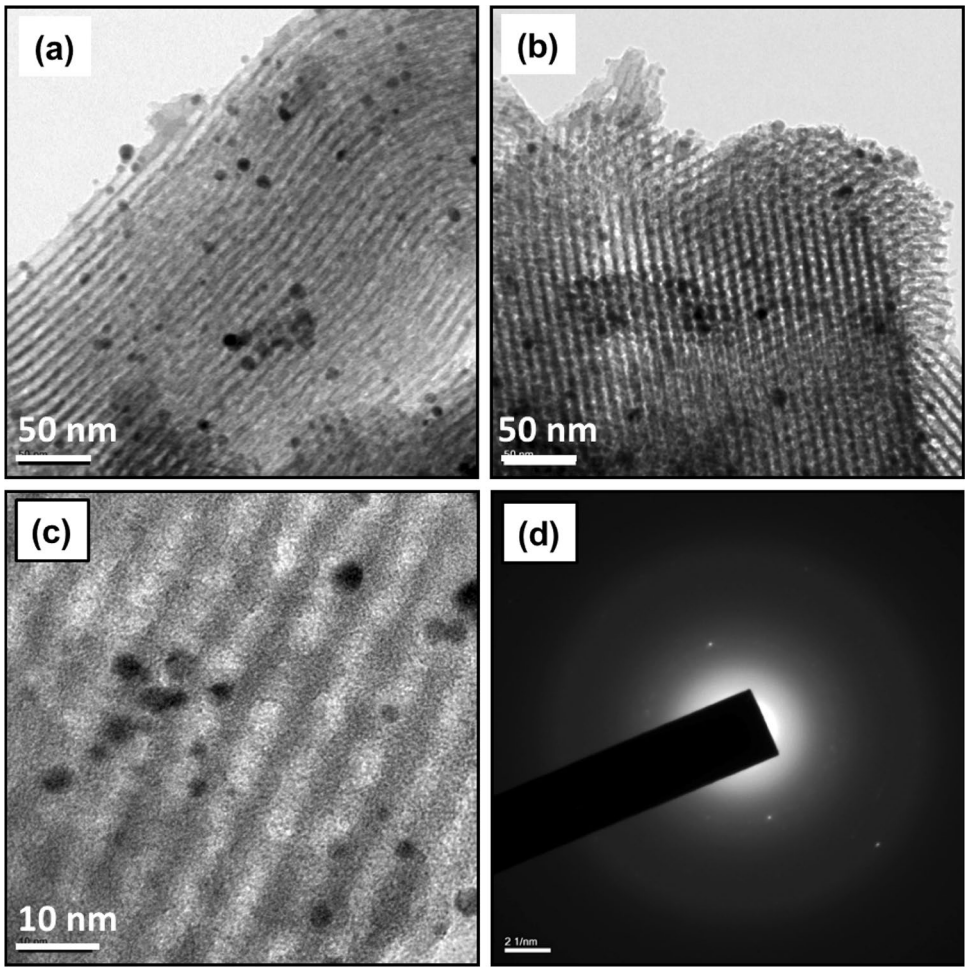

Fig. 6 HRTEM images of Cu/NH_2-SBA-15

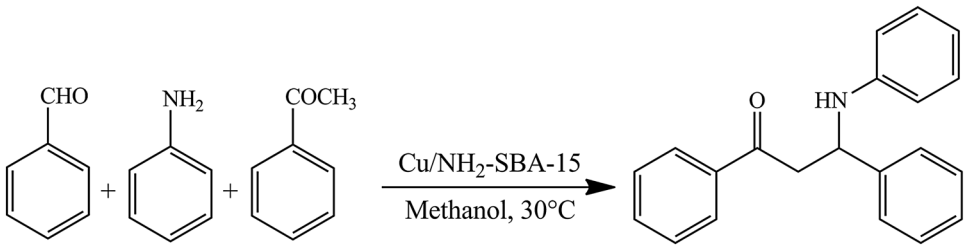

Scheme 1 Mannich type condensation of benzaldehyde, acetophenone and aniline in the presence of Cu/NH_2-SBA-15 catalyst

of SBA-15, make them act similar to nanoreactors. The amine functionalization of SBA-15 provides excellent support for the uniform dispersion of Cu NPs. Interestingly the pore walls seem to be unbroken even after loading Cu NPs. Also, the chances of Cu NP leaching during the course of the reaction will be prevented due to compact loading inside these pores.

In general, the amine functionalization on SBA-15, narrowed the pore size distribution in the range of 1-3 nm. Further, decrease in the pore size, volume and specific area is ascribed to the progressive blockage due to copper nanoparticles inside the pore channels of SBA-15. The obtained results are in agreement with the PXRD, FT-IR and HRTEM.

3.2 Efficiency of Cu/NH_2-SBA-15 Catalyst in Mannich Reaction

The catalytic performances of Cu/NH_2-SBA-15 catalyst are investigated in three-component Mannich reaction. In order to optimize the reaction conditions, acetophenone, benzaldehyde and aniline are selected as model reactants to provide Mannich base (1,3-Diphenyl-3-(phenylamino) propan-1-one compound) (Scheme 1). The reaction conditions such as solvents, reaction time and temperature are

Table 1 Cu/NH_2-SBA-15 catalysed three component Mannich type reactions of benzaldehyde, aniline and acetophenone in different solvents

Entry	Solvent	Yield[a]
1	Acetonitrile	40
2	Dichloromethane	20
3	Methanol	90
4	Water	10
5	*n*-Hexane	Trace
6	No solvent	–

Reaction conditions: benzaldehyde (1 mmol), acetophenone (1 mmol), aniline (1 mmol), solvent (5 mL), catalyst (50 mg), 30 °C, 10 h

[a]Isolated yield

Table 2 Mannich reaction of various aldehydes catalyst by Cu/NH_2-SBA-15

Entry	Aldehyde	Yield[a]
1	Benzaldehyde	90
2	4-Chlorobenzaldehyde	80
3	4-Methylbenzaldehyde	85
4	4-Methoxybenzaldehyde	71
5	2-Nitrobenzaldehyde	Trace
6	4-Bromobenzaldehyde	74

Reaction conditions: aromatic aldehyde (1 mmol), acetophenone (1 mmol), aniline (1 mmol), methanol (5 mL), catalyst (50 mg), 30 °C, 12 h

[a]Isolated yield

screened. For all reaction, the progress of the reaction was monitored and the products were confirmed by TLC and NMR respectively.

At different time intervals (up to 24 h) formation of product 1,3-diphenyl-3-(phenylamino)propan-1-one is examined. The catalyst has shown maximum yield of about 90% after 10 h. Further, only marginal increase in yield is noted while continuing the reaction up to 24 h. Noticeably, imine (bezaldehyde + aniline) type product was formed at lower reaction time (5 h) [35, 36]. However, in the absence of the catalyst, only 10% yield (imine) was formed even after 24 h. Similarly, increasing the catalyst amount (> 50 mg) did not improve the yield significantly. Furthermore, the reaction tested with pure amine functionalised SBA-15 (NH_2-SBA-15) yields 40% of Mannich base. Mondal et al. has reported that pure amino-functionalized mesoporous silica is an efficient base catalyst for the Knoevanagel condensation reaction [37]. These results suggest that the catalyst play a crucial role in the Mannich reaction. To understand the role of solvent, the reaction was carried out with different solvents, such as acetonitrile, dichloromethane, methanol, water and *n*-heptane, the results are summarized in Table 1. Notably, the product yield is higher for methanol (90%) than acetonitrile, water and dichloromethane solvents. Using, *n*-hexane a non-polar solvent, conversion is very low. There was no product yield noticed in solvent free reaction. Essentially, the solvent helps the reactants to conduct with the dispersed Cu^0 active sites, which resides in the mesopores. From the screened solvent systems, methanol is the solvent of choice for the Mannich reaction.

In addition, the high temperature could improve the reaction rate, but favor side reactions and the oxygenolysis of aldehydes and amine [13, 38]. Similar, type of observations was reported in literature. It is found that 30 °C is an appropriate condition for reaction. From the reaction optimization, we found that a maximum yield of 90% in 10 h was obtained in methanol at 30 °C in reflux condition. Kidwai et al. has reported the effects of Cu nanoparticle size on Mannich reaction. The maximum reaction rate has been observed for 20 nm sized particles, below this size tended to decrease in reaction rate [14]. However, in the present work, amine stabilized Cu-nanoparticles in the range of 5–10 nm size have shown good activity for the Mannich reaction.

The one-pot, three component Mannich reaction using various aromatic aldehydes with different substituted groups were tested with optimized reaction conditions and the results are summarized in Table 2. For all the substrates, different yields of the products are obtained within 12 h reaction time. Besides, the electron withdrawing (–Cl, –Br, $–NO_2$) and donating ($–CH_3$, $–OCH_3$) groups substituted benzaldehydes give higher yields. Particularly, substituted benzaldehyde with electron withdrawing or donating groups in *para* position result the products in good yields (70–80%) whereas *ortho*-substituted benzaldehyde (2-nitrobenzaldehyde) provided no yield due to steric effects and imine formation [35].

After completion of the reaction Cu/NH_2-SBA-15 was filtered from the reaction mixture, washed by acetone and dried at 100 °C for 6 h. The reusability of the catalyst is also tested for Mannich reaction. Before next reaction, the catalyst is activated at 120 °C for 2 h in N_2 atm. From the reaction results, it was found that the catalyst can be recycled and reused for three cycles without much loss of efficiency. This indicates that Cu/NH_2-SBA-15 is an efficient heterogeneous catalyst for Mannich reaction.

3.3 Reduction of Dyes Using Mesoporous Cu/NH_2-SBA-15 as Catalyst

The catalytic nature of mesoporous Cu/NH_2-SBA-15 was tested for MG, PR and BPB reduction using $NaBH_4$ as reducing agent. All the dye molecules contain triphenyl methane backbones and are grouped depending on the nature of the substituents on their hydrocarbon triphenyl methane. Notably, these dyes were used in textile, dyeing, food,

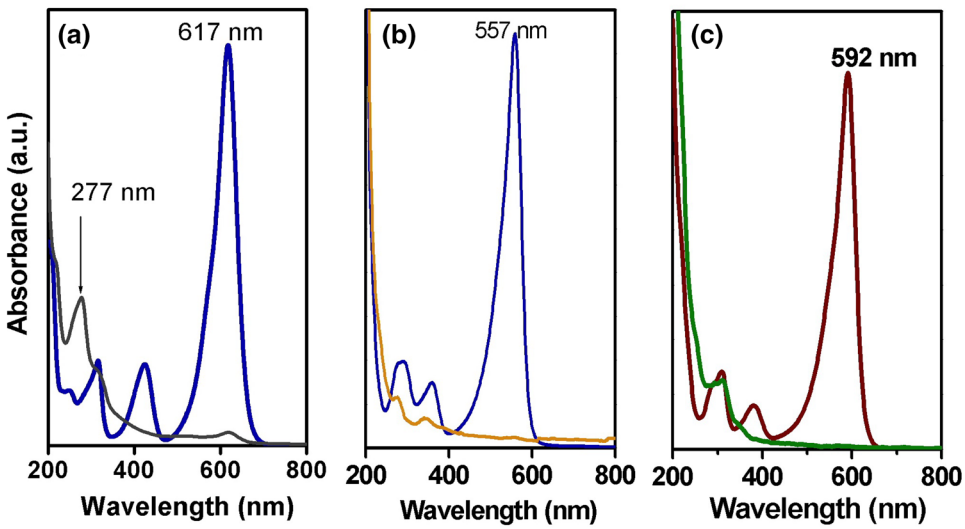

Fig. 7 UV–visible absorption spectra for before and after reduction with Cu/NH_2-SBA-15: **a** MG, **b** PR, and **c** BPB

cosmetic industries and also as biological stain in pharmaceuticals. However, those types of dyes are toxic to aquatic organisms and are considered to be potential mutagenesis and carcinogenesis agents to mammalian cells. To understand the role of the substituents and the nature of dyes in the mechanism of reduction, diamino (MG) cationic and phenol derivative (PR, BPB) anionic dyes were selected. The reaction was monitored and analyzed using UV–visible spectrometer on the respective chromophoric λ_{max} values of the dyes. The reduction kinetics of these dyes was followed on their chromophoric absorptions at 617, 557 and 592 nm for MG, PR and BPB, respectively. These absorption maxima were ascribed to the CT (π–π^*) transition within the dye molecules. When catalytic amount of Cu/NH_2-SBA-15 was added to the reaction mixture containing the dye molecule and BH_4^-, the intense peak corresponding to MG, PR and BPB disappears rapidly with the concomitant appearance of a new peak/shift depending upon the nature of the dyes (Fig. 7). This change is evident from the visible color change from green, red and blue to colorless for MG, PR and BPB respectively. Addition of excess $NaBH_4$ to the dye solutions does not cause any of these spectral changes. Only in the presence of catalytic amount of Cu/NH_2-SBA-15 the spectral changes can be observed. As soon as catalyst was added, leuco form of dyes were formed as confirmed from the appearance of new peak for MG (277 nm) and hypsochromic shift for PR (358 and 284 nm to 339 and 269 nm). About, 98% of dye was reduced in about 5 min.

To apprehend the role of Cu nanoparticles, the reactions were conducted in the presence and absence of Cu/NH_2-SBA-15, NH_2-SBA-15, SBA-15 and $NaBH_4$. It is well noted that in the absence of Cu/NH_2-SBA-15 alone, the λ_{max} values are unaltered, indicating the importance of Cu NPs in the reduction of dyes. Besides, the relative order of reduction of triphenyl methane dyes is found to be MG > PR > BPB. Interestingly, MG is reduced 4 times faster than PR and 8 times faster than BPB. The MG being a cationic dye is attracted easily to the Cu–BH_4^- complex in Cu/NH_2-SBA-15. The anionic dyes PR and BPB are attached to the protonated amino groups present on the surface of SBA-15. While comparing the anionic dyes PR and BPB, bulky bromo substituents in bromophenol blue may cause steric hindrance for effective binding on Cu/NH_2-SBA-15 catalyst surface. Hence the rate of reduction of bromophenol blue may be lower than phenol red. The detailed mechanisms for the dye reduction are given in the supplementary information.

4 Conclusion

Mesoporous Cu/NH_2-SBA-15 was synthesised by a simple impregnation method and characterised systematically. The results prove that copper nanoparticles were dispersed in the mesochannels and surface of amine functionalised hexagonal lamelliform SBA-15 with high surface area, tunable pore size and short vertical channels. Copper nanoparticles present in mesochannels of NH_2-SBA-15 acts as nonreactor for the catalytic reactions and prevented from leaching. The catalytic activity of Cu/NH_2-SBA-15 in Mannich reaction enabled high yield of β-amino carbonyl compounds (~ 70 to 80% yield). The reaction procedure could also be applied for aromatic aldehydes, aromatic ketones and amines with both electron-donating and electron-withdrawing substituents. Similarly, the catalyst revealed the excellent reduction of triphenyl methane dyes with $NaBH_4$ to their corresponding leuco forms at 5 min of reaction time. Therefore Cu/NH_2-SBA-15 proved to be

potential candidate for the synthesis of Mannich reaction and dye reduction reactions.

Compliance with Ethical Standards

Conflict of interest The authors declare that they have no conflict of interest.

References

1. C. Mannich, W. Krösche, Ueber ein Kondensationsprodukt aus Formaldehyd, Ammoniak und Antipyrin. Arch. Pharm. Pharm. Med. Chem. **250**, 647–667 (1912). https://doi.org/10.1002/ardp.19122500151
2. M. Tramontini, L. Angiolini, *Mannich bases-chemistry and uses*, vol. 5 (CRC Press, Boca Raton, 1994)
3. M. Arend, B. Westermann, N. Risch, Modern variants of the Mannich reaction. Angew. Chem. Int. Ed. **37**(8), 1044–1070 (1998). https://doi.org/10.1002/(sici)1521-3773(19980504)37:8%3c1044:aid-anie1044%3e3.0.co;2-e
4. W.N. Speckamp, M.J. Moolenaar, New developments in the chemistry of N-acyliminium ions and related intermediates. Tetrahedron **56**(24), 3817–3856 (2000). https://doi.org/10.1016/S0040-4020(00)00159-9
5. B.M. Trost, L.R. Terrell, A direct catalytic asymmetric Mannich-type reaction to syn-amino alcohols. J. Am. Chem. Soc. **125**(2), 338–339 (2003). https://doi.org/10.1021/ja028782e
6. S. Matsunaga, N. Kumagai, S. Harada, M. Shibasaki, Anti-Selective direct catalytic asymmetric Mannich-type reaction of hydroxyketone providing β-amino alcohols. J. Am. Chem. Soc. **125**(16), 4712–4713 (2003). https://doi.org/10.1021/ja034787f
7. T. Akiyama, K. Matsuda, K. Fuchibe, HCl-catalyzed stereoselective Mannich reaction in H_2O-SDS system. Synlett (2005). https://doi.org/10.1055/s-2004-836062
8. T. Akiyama, J. Takaya, H. Kagoshima, One-pot Mannich-type reaction in water: HBF4 catalyzed condensation of aldehydes, amines, and silyl enolates for the synthesis of β-amino carbonyl compounds. Synlett **15**(09), 1426–1428 (1999)
9. M. Periasamy, S. Suresh, S.S. Ganesan, Stereoselective synthesis of syn-β-amino esters using the TiCl 4/R 3 N reagent system. Tetrahedron Lett. **46**(33), 5521–5524 (2005). https://doi.org/10.1016/j.tetlet.2005.06.048
10. D. Prukała, New compounds via Mannich reaction of cytosine, paraformaldehyde and cyclic secondary amines. Tetrahedron Lett. **47**(51), 9045–9047 (2006). https://doi.org/10.1016/j.tetlet.2006.10.117
11. E. Takahashi, H. Fujisawa, T. Mukaiyama, Lithium acetate-catalyzed Mannich-type reaction between trimethylsilyl enolates and aldimines in a water-containing DMF. Chem. Lett. **33**(7), 936–937 (2004). https://doi.org/10.1246/cl.2004.936
12. M. Kidwai, D. Bhatnagar, N.K. Mishra, V. Bansal, CAN catalyzed synthesis of β-amino carbonyl compounds via Mannich reaction in PEG. Catal. Commun. **9**(15), 2547–2549 (2008). https://doi.org/10.1016/j.catcom.2008.07.010
13. R.K. Sharma, D. Rawat, G. Gaba, Inorganic–organic hybrid silica based tin (II) catalyst: synthesis, characterization and application in one-pot three-component Mannich reaction. Catal. Commun. **19**, 31–36 (2012). https://doi.org/10.1016/j.catcom.2011.12.006
14. M. Kidwai, N.K. Mishra, V. Bansal, A. Kumar, S. Mozumdar, Novel one-pot Cu-nanoparticles-catalyzed Mannich reaction. Tetrahedron Lett. **50**(12), 1355–1358 (2009). https://doi.org/10.1016/j.tetlet.2009.01.031
15. B. White, M. Yin, A. Hall, D. Le, S. Stolbov, T. Rahman, S. O'Brien, Complete CO oxidation over Cu_2O nanoparticles supported on silica gel. Nano Lett. **6**(9), 2095–2098 (2006). https://doi.org/10.1021/nl061457v
16. H. Berndt, A. Martin, A. Brückner, E. Schreier, D. Müller, H. Kosslick, G.U. Wolf, B.J. Lücke, Structure and catalytic properties of VOx/MCM materials for the partial oxidation of methane to formaldehyde. J. Catal. **191**(2), 384–400 (2000). https://doi.org/10.1006/jcat.1999.2786
17. V. Fornés, C. Lopez, H.H. Lopez, A. Martınez, Catalytic performance of mesoporous VOx/SBA-15 catalysts for the partial oxidation of methane to formaldehyde. Appl. Catal. A **249**(2), 345–354 (2003). https://doi.org/10.1016/S0926-860X(03)00226-6
18. M. Baltes, K. Cassiers, P. Van Der Voort, B.M. Weckhuysen, R.A. Schoonheydt, E.F. Vansant, MCM-48-supported vanadium oxide catalysts, prepared by the molecular designed dispersion of VO (acac) 2: a detailed study of the highly reactive MCM-48 surface and the structure and activity of the deposited VOx. J. Catal. **197**(1), 160–171 (2001). https://doi.org/10.1006/jcat.2000.3066
19. G. Du, S. Lim, M. Pinault, C. Wang, F. Fang, L. Pfefferle, G.L. Haller, Synthesis, characterization, and catalytic performance of highly dispersed vanadium grafted SBA-15 catalyst. J. Catal. **253**(1), 74–90 (2008). https://doi.org/10.1016/j.jcat.2007.10.019
20. F. Kleitz, F. Berube, R. Guillet-Nicolas, C.M. Yang, M. Thommes, Probing adsorption, pore condensation, and hysteresis behavior of pure fluids in three-dimensional cubic mesoporous KIT-6 silica. J. Phys. Chem. C **114**(20), 9344–9355 (2010). https://doi.org/10.1021/jp909836v
21. D. Zhao, J. Sun, Q. Li, G.D. Stucky, Morphological control of highly ordered mesoporous silica SBA-15. Chem. Mater. **12**(2), 275–279 (2000). https://doi.org/10.1021/cm9911363
22. C.H. Tu, A.Q. Wang, M.Y. Zheng, X.D. Wang, T. Zhang, Factors influencing the catalytic activity of SBA-15-supported copper nanoparticles in CO oxidation. Appl. Catal. A **297**(1), 40–47 (2006). https://doi.org/10.1016/j.apcata.2005.08.035
23. K. Yoshida, C. Gonzalez-Arellano, R. Luque, P.L. Gai, Efficient hydrogenation of carbonyl compounds using low-loaded supported copper nanoparticles under microwave irradiation. Appl. Catal. A **379**(1–2), 38–44 (2010). https://doi.org/10.1016/j.apcata.2010.02.028
24. C.M. Chanquía, K. Sapag, E. Rodríguez-Castellón, E.R. Herrero, G.A. Eimer, Nature and location of copper nanospecies in mesoporous molecular sieves. J. Phys. Chem. C **114**(3), 1481–1490 (2010). https://doi.org/10.1021/jp9094529
25. B.K. Ghosh, S. Hazra, B. Naik, N.N. Ghosh, Preparation of Cu nanoparticle loaded SBA-15 and their excellent catalytic activity in reduction of variety of dyes. Powder Technol. **269**, 371–378 (2015). https://doi.org/10.1016/j.powtec.2014.09.027
26. D. Zhao, J. Feng, Q. Huo, N. Melosh, G.H. Fredrickson, B.F. Chmelka, G.D. Stucky, Triblock copolymer syntheses of mesoporous silica with periodic 50 to 300 angstrom pores. Science **279**(5350), 548–552 (1998). https://doi.org/10.1126/science.279.5350.548
27. S. Anbu Anjugam Vandarkuzhali, S. Karthikeyan, B. Viswanathan, M.P. Pachamuthu, Arachis hypogaea derived activated carbon/Pt catalyst: reduction of organic dyes. Surf. Interfaces **13**, 101–111 (2018). https://doi.org/10.1016/j.surfin.2018.07.005
28. N.A. Brunelli, K. Venkatasubbaiah, C.W. Jones, Cooperative catalysis with acid–base bifunctional mesoporous silica: impact of grafting and co-condensation synthesis methods on material structure and catalytic properties. Chem. Mater. **24**(13), 2433–2442 (2012). https://doi.org/10.1021/cm300753z

29. M.P. Pachamuthu, S. Karthikeyan, R. Maheswari, A.F. Lee, A. Ramanathan, Fenton-like degradation of Bisphenol A catalyzed by mesoporous Cu/TUD-1. Appl. Surf. Sci. **393**, 67–73 (2017). https://doi.org/10.1016/j.apsusc.2016.09.162
30. L. Chen, J. Hu, Z. Qi, Y. Fang, R. Richards, Gold nanoparticles intercalated into the walls of mesoporous silica as a versatile redox catalyst. Ind. Eng. Chem. Res. **50**(24), 13642–13649 (2011). https://doi.org/10.1021/ie200606t
31. R. Al-Oweini, H. El-Rossy, Synthesis and characterization by FTIR spectroscopy of silica aerogels prepared using several Si(OR)4 and R″Si(OR′)3 precursors. J. Mol. Struct. **919**, 140–145 (2009). https://doi.org/10.1016/j.molstruc.2008.08.025
32. B.L. Newalkar, S. Komarneni, Control over microporosity of ordered microporous–mesoporous silica SBA-15 framework under microwave-hydrothermal conditions: effect of salt addition. Chem. Mater. **13**(12), 4573–4579 (2001). https://doi.org/10.1021/cm010 3038
33. Y. Zhu, H. Li, Q. Zheng, J. Xu, X. Li, Amine-functionalized SBA-15 with uniform morphology and well-defined mesostructure for highly sensitive chemosensors to detect formaldehyde vapor. Langmuir **28**(20), 7843–7850 (2012). https://doi.org/10.1021/la300560j
34. Y.F. Shi, Y. Meng, D.H. Chen, S.J. Cheng, P. Chen, H.F. Yang, Y. Wan, D.Y. Zhao, Highly ordered mesoporous silicon carbide ceramics with large surface areas and high stability. J. Mater. Chem. **16**, 1511–1519 (2006). https://doi.org/10.1002/adfm.20050 0643
35. M.P. Pachamuthu, K. Shanthi, R. Luque, A. Ramanathan, SnTUD-1: a solid acid catalyst for three component coupling reactions at room temperature. RSC Green Chem. **15**, 2158–2166 (2013). https://doi.org/10.1039/C3GC40792F
36. T.P. Loh, S.K.W. Liung, K.L. Tan, L.L. Wei, Three component synthesis of b-amino carbonyl compounds using indium trichloride-catalyzed one-pot mannich-type reaction in water. Tetrahedron **56**, 3227–3323 (2000). https://doi.org/10.1016/S0040-4020(00)00221-0
37. J. Mondal, A. Modak, A. Bhaumik, Highly efficient mesoporous base catalyzed Knoevenagel condensation of different aromatic aldehydes with malononitrile and subsequent noncatalytic Diels–Alder reactions. J. Mol. Catal. A **335**, 236–241 (2011). https://doi.org/10.1016/j.molcata.2010.11.039
38. L. Hua, Z. Hong-yao, S. Hua-wu, Bismuth(III) chloride-catalyzed one-pot Mannich reaction: three-component synthesis of β-amino carbonyl compounds. Tetrahedron Lett. **50**, 6858–6860 (2009). https://doi.org/10.1016/j.tetlet.2009.09.131
39. B.K. Ghosh, S. Hazra, B. Naik, N.N. Ghosh, Preparation of Cu nanoparticle loaded SBA-15 and their excellent catalytic activity in reduction of variety of dyes. Powder Technol. **269**, 371–378 (2015). https://doi.org/10.1016/j.powtec.2014.09.027

Affiliations

S. Anbu Anjugam Vandarkuzhali[1] · B. Viswanathan[1] · M. P. Pachamuthu[2] · S. Chandra Kishore[3]

✉ B. Viswanathan
bviswanathan@gmail.com

✉ M. P. Pachamuthu
pachachem@gmail.com; pachamuthu@bitsathy.ac.in

[1] National Center for Catalysis Research, Indian Institute of Technology Madras, Chennai, Tamil Nadu 600036, India

[2] Department of Chemistry, Bannari Amman Institute of Technology, Sathyamangalam, Erode 638401, India

[3] University of Information Science and Technology "St. Paul the Apostle", Partizanska bb, 6000 Ohrid, Republic of Macedonia